**S. Parneix**
Post-Doctoral Fellow,
Center for Turbulence Research,
Stanford University,
Stanford CA, 94305-3030

**D. Laurence**
Senior Research Engineer,
Electricité de France, DER,
Laboratoire National d'Hydraulique,
6 quai Watier, 78400 Chatou, France

**P. A. Durbin**
Professor,
Mechanical Engineering,
Stanford University,
Stanford CA, 94305-3030

# A Procedure for Using DNS Databases

*A second moment closure (SMC) computation is compared in detail with the direct numerical simulation (DNS) data of Le et al. (1997) for the backstep flow at Re = 5100 in an attempt to understand why the intensity of the backflow and, consequently, the friction coefficient in the recirculation bubble are under-estimated. The data show that this recirculation bubble is far from being laminar except in the very near wall layer. A novel "differential a priori" procedure was used, in which the full transport equation for one isolated component of the Reynolds stress tensor was solved using DNS data as input. Conclusions are then different from what would have been deduced by comparing a full simulation to a DNS. In particular, the $\epsilon$-equation, usually blamed for faults in model predictions, has been found to give excellent results in this case. In fact, the main problem comes from the $\overline{uv}$-equation which predicts a too high turbulent force. A modification, by including the gradients of mean flow in the transport model, has then been attempted and has cured 50 percent of the backflow discrepancy.*

## 1 Introduction

A commonly given motive for direct numerical simulation (DNS) of turbulent flow is to provide data that might be of value to modelers. However, in the case of nonhomogeneous turbulence, only the one-dimensional data from fully-developed channel flow has received wide-spread use (Rodi and Mansour, 1993). That data set has lived up to promise, but simulations of more complex geometries have not proved as useful.

The geometrical simplicity of channel flow does not permit one to assess many of the essential properties of turbulence models. On a mathematical level, the single-point moment equations are ordinary differential equations in channel flow; on a physical level, the phenomenon of flow separation is not addressed by this case.

The manner in which DNS data has been utilized by modelers also has not exploited its potential. The standard "assessment" of a pressure-strain model has consisted of plugging DNS data into the algebraic formulas of the model, then comparing the result to other DNS data. This is not a proper assessment of a transport closure model: the model is phrased as a set of partial differential equations and boundary conditions, not as an algebraic formula, so the plug-in exercise can be misleading. Moreover, one important problem with such a technique is that, even if a "perfect" equation is found for every term of the global budgets (which means that the modeled equation fits perfectly with the DNS data), the general convergence of the global system has not been included in the study, and the resulting model can be numerically unstable. Such terms like dissipation or transport of Reynolds stresses may also be not well enough resolved, even by recent DNS, for an accurate and complete analysis term by term. It is more sensible to treat DNS data as conventional experimental data and simply compare it to *solutions* of the model.

In this paper, we propose an intermediate level of testing: the differential nature of the model is respected, but the DNS data is plugged into the model. Our motivation is to isolate individual aspects of the closure. For instance, if the mean flow and the Reynolds stresses are given by DNS data, does the $k - \epsilon$ system of the Second Moment Closure equations (which is, of course, different from the classical $k - \epsilon$ model) predict $k$ and $\epsilon$ correctly? The $\epsilon$-equation is commonly blamed for faults in model predictions: can this be substantiated by isolating that equation from other closure assumptions? In fact, when we isolated the $\epsilon$-equation by utilizing DNS data from the Le et al. (1997) simulation of flow over a backward facing step, we found the $\epsilon$-equation to do an admirable job. The results presented herein do not confirm the conventional wisdom.

To the best of our knowledge, only Hanjalic (1994) has previously used a preliminary version of the present method. Hanjalic did not actually describe the method or its significance; however, the caption of his Fig. 13 indicates that the $\epsilon$-equation was solved using the Reynolds stresses $\overline{u_i u_j}$ and the mean velocity $U$ from the DNS of a channel flow. In essence this embodies the idea of differential a priori testing: test the model by using DNS data fields, but still solve a full transport equation for the turbulence statistics. The present paper presents the first comprehensive, two-dimensional use of this technique. We have used a RANS code to obtain solutions to the turbulence transport equations.

## 2 Methodology

An "a priori" test is one in which a model is assessed outside of its full predictive context. The objective of a priori testing is to remove ambiguities or inaccuracies that occur in solutions of the full set of equations. These include numerical errors and inaccuracies in terms additional to those being tested. Numerical inaccuracy motivates a priori tests of LES subgrid closures; modeling inaccuracy motivates the present application to RANS closure.

All a priori testing suffers the danger of not judging the true mathematical role of the model. A model for the redistribution term of the Reynolds-stress transport equation is a formula to be used in a set of parabolic partial differential equations. It should be judged by its effect on the dependent variable, $\overline{u_i u_j}$, of those equations. This entails solving the transport model. To isolate the turbulence model, the mean flow field can be taken from a DNS data base; we will use the backstep simulation data of Le et al. (1997). Furthermore, each component of the transport equations can be isolated by prescribing the other components of $\overline{u_i u_j}$ via DNS fields. The isolated component must be solved in full.

Our method is to solve the partial differential equations of the turbulence model numerically, with certain fields prescribed

Contributed by the Fluids Engineering Division for publication in the JOURNAL OF FLUIDS ENGINEERING. Manuscript received by the Fluids Engineering Division January 22, 1997; revised manuscript received May 27, 1997. Associate Technical Editor: P. M. Sockol.

  

by DNS data. In general, the distribution of grid points for a DNS is not optimal for RANS, so we have interpolated the DNS fields onto a RANS grid; bilinear interpolation was used. The 770 × 194 DNS grid of Le et al. was uniform in $x$ and stretched in $y$. The RANS grid is nonuniform in both directions and consisted of 120 × 120 cells, refined near the walls and around the corner of the step. It covered the region $x/h = -3$ to 30 and $y/h = 0$ to 6, $x = 0$ being the location of the sudden expansion, $h$ being the step height and $y = 6h$ being the center of the channel. All RANS computations were performed with a general geometry, finite difference code developed by Rogers and Kwak (1990). The spatial discretization of convective terms was via a third-order, upwind biased scheme; diffusion terms were central differenced. Solutions were checked for grid-independence on a grid twice finer in both directions: the results were graphically indistinguishable from those presented herein. Inlet profiles of mean velocities, Reynolds stresses and dissipation were also taken from the DNS and imposed as the inlet conditions of all the following computations.

This new a priori method can be applied to the $k$ and $\epsilon$ equations, which are a subset of the full Second Moment Closure equations (see the Appendix for the complete SMC model):

$$U_i^{\mathrm{DNS}}\partial_i k = \mathcal{P}^{\mathrm{DNS}} - \epsilon + \partial_i(\nu + \nu_{T_{ij}})\partial_j k$$

$$U_i^{\mathrm{DNS}}\partial_i \epsilon = \frac{C'_{\epsilon_1}\mathcal{P}^{\mathrm{DNS}} - C_{\epsilon_2}\epsilon}{T} + \partial_i(\nu + \nu_{T_{ij}})\partial_j \epsilon \qquad (1)$$

with $\nu_{T_{ij}} = C_\mu T \overline{u_i u_j}^{\mathrm{DNS}}$ and boundary conditions $k = \partial_n k = 0$ on no-slip walls. The production term uses the exact definition

$$\mathcal{P}^{\mathrm{DNS}} = -\overline{u_i u_j}^{\mathrm{DNS}}\partial_j U_i^{\mathrm{DNS}}. \qquad (2)$$

The turbulence time-scale

$$T = \sqrt{\frac{k^2}{\epsilon^2} + 36\frac{\nu}{\epsilon}}$$

involves the dependent variables, so it was computed as part of the a priori test. The terms in (1) with "DNS" superscript are ensemble averaged DNS fields that were interpolated onto the RANS grid; $k$ and $\epsilon$ were obtained by solving these equations.

## 3 Full Computations

In addition to the a priori tests, a full SMC, RANS computation was performed. The full computation shows some areas in which improvements to the model are desired. The SSG redistribution model (Speziale et al., 1991) was used in conjunction with the elliptic relaxation method for treating wall effects (Durbin, 1993; Wizman et al., 1996), see the Appendix. The specifics of the modeling are not crucial here; our results are likely to be representative of the class of SMC's based on the general quasi-linear form, (A.5). The model constants were originally calibrated using DNS and experimental data for channel flow, zero pressure gradient boundary layers (Durbin, 1993) and homogeneous flows (Speziale et al., 1991). That model was directly applied to the backstep flow, without further modification. All the equations and constants used for this computation can be found in the Appendix.

Figure 1 shows the predicted streamlines compared to the DNS data. One can observe that the reattachment length is very well predicted and a secondary bubble is found. The flow seems to have a correct behavior near the reattachment point: it does not show the anomalous streamline pattern that has been found in other computations (Hanjalic, 1996, with the SSG pressure-strain model). Because of these previous results, we did a careful grid refinement study to verify that the present solution does not contain the spurious streamline pattern near reattachment

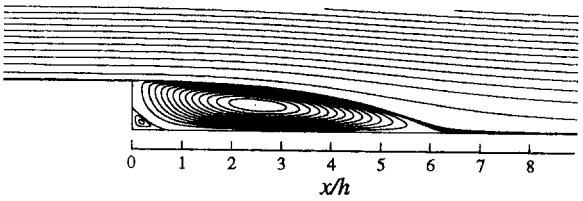


Fig. 1(*a*) Streamlines, second moment closure

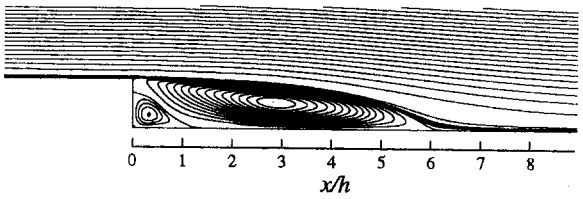


Fig. 1(*b*) Streamlines, DNS

that Hanjalic obtained. The elliptic relaxation method might be the source of the improvement.

However, the size of the secondary, corner bubble is much smaller in the computation than in the data. This defect seems to be linked to an under-prediction of the maximum friction coefficient in the backflow (Fig. 2(*a*)). By looking to the profiles of the streamwise mean velocity (Fig. 2(*b*)), one can observe that the overall features of the mean flow are reproduced, but the intensity of the backflow is missed by almost a factor of 2 at $x/h = 4$. Note that this specific problem seems to be common to every existing second moment closure (SMC) model, whatever near-wall formulation is used (low-Reynolds number, wall function or elliptic relaxation). Also, as with all existing turbulence models, including eddy viscosity models, the recovery after reattachment is too slow. The friction coefficient distribution shows similar discrepancies (too slow near-wall flow) both upstream and downstream the reattachment point, but we do not know if these two problems (too slow backflow and too slow recovery) are linked.

Figure 3 presents profiles of the computed normal component of the mean velocity $V$. The $V$-profiles at $x/h = 0.1$ and 2 confirm the distribution of the friction coefficient: the intensity of the two bubbles is severly under-estimated. By looking at the profiles before reattachment, one can observe that $V$ is also under-estimated in the shear layer by about 15 percent. In fact, all the problems can be linked together by noting that more entrainment in the shear layer would lead to a more intense main recirculation, leading to a bigger and more intense secondary bubble. However, a modification of the backflow would also change the pressure distribution and thereby influence the velocity distribution in the shear layer.

## 4 A Priori Tests

A standard way of analyzing a DNS database consists in using the full DNS data to compute the distribution of some important variables, like the turbulent Reynolds number—$\mathrm{Re}_t = k^2/(\nu\epsilon)$—in order to understand the main physical features of the flow or to get new ideas for modeling. Figure 4, showing $\mathrm{Re}_t$ and the budget of the U-momentum equation in the middle of the recirculation ($x/h = 4$), presents an example of such a study. In their experiments, Jovic and Driver (1995) found that the minimum of $C_f$ follows a "laminar-like" law: $C_{f_{min}} = -0.19\mathrm{Re}_h^{-0.5}$ for Reynolds numbers between 5000 and 50,000. However, $\mathrm{Re}_t$, which represents about ten times the ratio between the turbulent viscosity and the molecular viscosity, is in the range 200–800 in the whole domain, including the bubble (of course, it goes to 0 at the wall). Clearly the flow is fully turbulent; the $\mathrm{Re}_h^{-0.5}$ fit does not imply a laminar recirculation

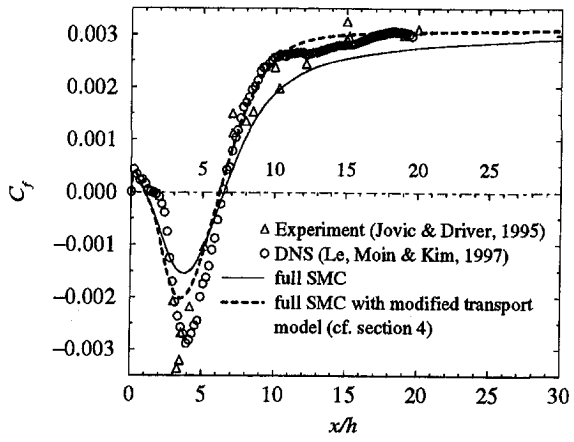


Fig. 2(*a*) Friction coefficient

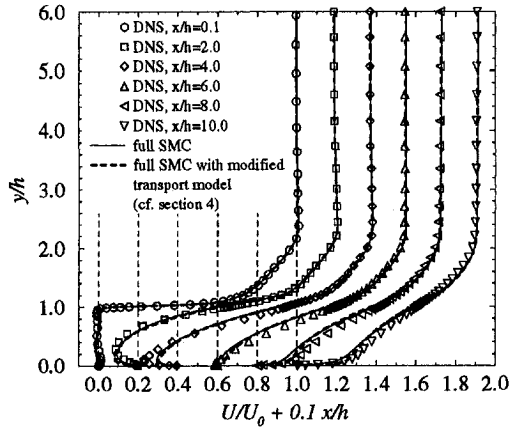


Fig. 2(*b*) *U* profiles

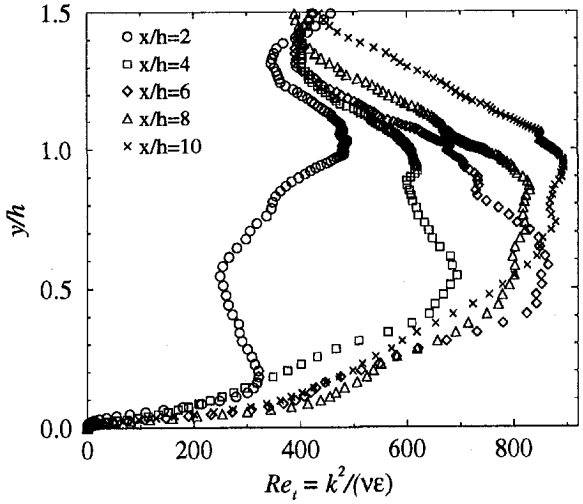


Fig. 4(*a*) DNS $Re_t$ profiles

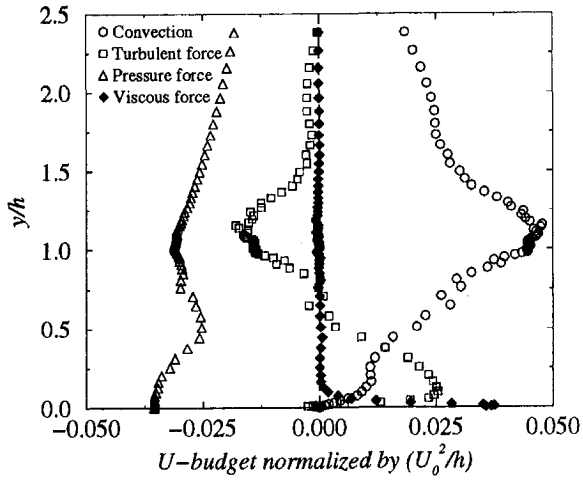


Fig. 4(*b*) *U*-momentum budget at station $x/h = 4$ (middle of the recirculation)

bubble. If one is still not completely sure of the turbulent nature of this recirculation, it becomes obvious by looking at the $U$-momentum budget (Fig. 4($b$)): at station $x/h = 4$, the Reynolds stress gradients dominate the viscous force in the whole bubble, except very near the wall, well below the maximum of the reverse flow.

It is possible to go further in the investigation of a DNS database: in the present case by utilizing the full DNS statistical fields to assess closure models. An overall comparison between full RANS computations and a priori tests explains why an analysis using only the full computation may lead to erroneous conclusions. For example, the known dependence of shear layer growth on the $\epsilon$-equation has lead to shortcomings of the full predictions being blamed on that equation. To judge the truth of this accusation, one might perform a parametric study on the model constants (we did so, and our efforts in that direction did not suggest that the $\epsilon$ model was the culprit). The a priori method provides a more refined test.

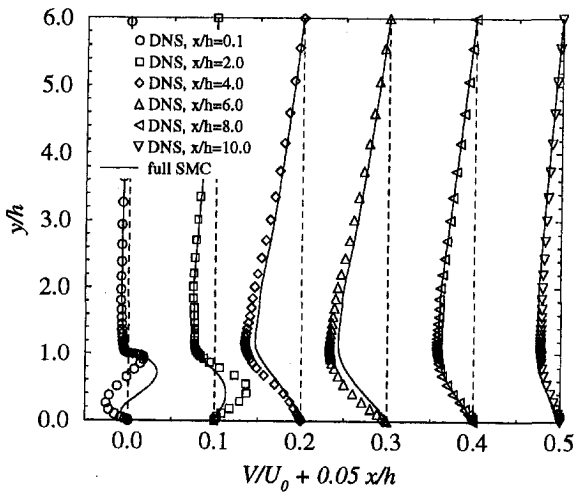


Fig. 3 *V* profiles

Figures 5 and 6 show a full RANS computation and an a priori "$k - \epsilon$" subsystem computation side by side (again, this is not the $k - \epsilon$ model, but the $k$ and $\epsilon$ equations coming from the SMC model). It can be seen (Figs. 5($b$) and 6($b$)) that when the correct mean flow convection velocity and production rate are given via DNS, the $k - \epsilon$ equations of the Second Moment Closure give good predictions. When we solved the $\epsilon$-equation separately, with $k$ given by DNS fields (Eq. (1)), results very similar to Figs. 6 were found (cf. Fig. 7($a$)).

This is an interesting test because the dissipation $\epsilon$ is usually considered as the weak point of any turbulence model. In fact, the derivation of the $\epsilon$-equation relies mainly on intuition, so most of the shortcomings of turbulence models were thought to be in this equation—and most of the modifications of turbulence models were done to it. In this study, we used the "primitive" $\epsilon$-equation, derived by Hanjalic and Launder (1972) with only two small modifications: $\epsilon/k$ has been replaced by the

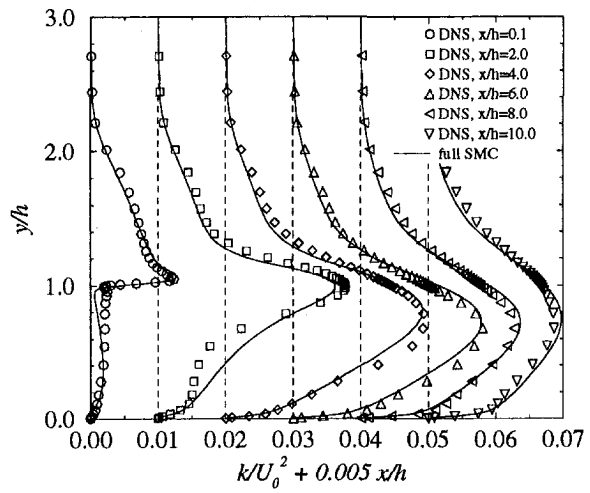


**Fig. 5(*a*) *k* profiles, full computation**

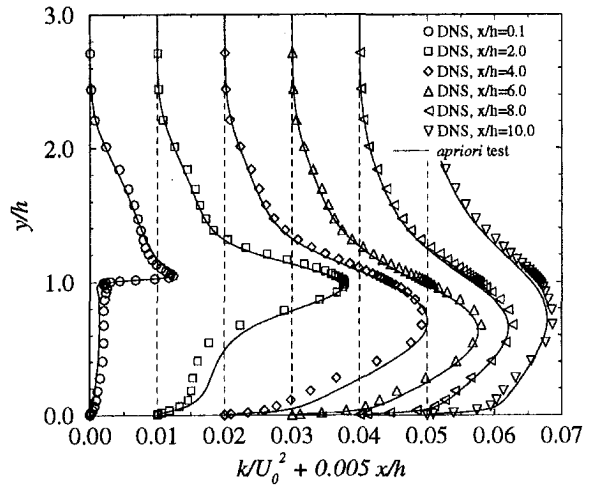


**Fig. 5(*b*) *k* profiles, a priori test**

inverse of the time scale $1/T$ (Durbin, 1993), and an extra-production term was included into $C_{\epsilon_1}$ to take into account the anisotropic wall effect (Parneix et al., 1996). In Eq. (1)

$$C'_{\epsilon_1} = C_{\epsilon_1}\left(1 + \tfrac{1}{30}\sqrt{\mathcal{P}_k/\mathcal{P}}\right) \qquad (3)$$

where $\mathcal{P}_k = 0.09(k^2/\epsilon)|S|^2$ is the production term that appears in the $k-\epsilon$ model and $\mathcal{P}$ is the exact Reynolds-stress production ($\mathcal{P} = -\overline{u_i u_k}\partial_k U_i$). This term is a generalization of the formulation $C'_{\epsilon_1} = C_{\epsilon_1}(1+\frac{1}{30}\sqrt{k/v^2})$, introduced by Durbin and Laurence (1996). It increases the production of $\epsilon$ in the near-wall region, thus decreasing the peak of the turbulent kinetic energy. The term $C'_{\epsilon_1} = C_{\epsilon_1} + a_1\mathcal{P}/\epsilon$ has sometimes been used for this same purpose, but the present method is more computationally stable in complex configurations.

When we fixed all the other variables at their DNS values (including $k$) and solved this equation, the results were surprisingly good, especially in the recirculation and in the recovery regions (cf. Fig. 7(*a*)). It is interesting to see whether the extra-term introduced in Eq. (3) has a strong influence or not on these results. Figure 7(*b*) presents the $k$-profiles computed through an a priori test ($k$ ans $\epsilon$ were solved together) without this extra-production term $\mathcal{P}_k/\mathcal{P}$ in the $\epsilon$-equation. The turbulent kinetic energy is then increased in the boundary layer, upstream from the step; this over-estimation is diffused in the shear-layer and in the recirculation by turbulent transport (higher levels than with the extra-term active, compare to Fig. 5(*b*)). Also, the peak of $k$, which starts to appear near the wall in the downstream recovery region seems to be over-estimated. Overall the influence is quite small and only affects the near-wall region. Indeed, when $\epsilon$ is solved alone with $k$ interpolated from the DNS, the $\epsilon$ profiles do not show any major difference with or without the extra-term of (3).

Given these results, it is difficult to believe that only a modification of the $\epsilon$-equation will cure all the problems, and especially the under-prediction of the backflow and rate of recovery. Although it is true that the reattachment length is sensitive to the difference $(C_{\epsilon_2} - C_{\epsilon_1})$, the origin of this seems to lie in the shear layer, where the dependence of the growth rate on $(C_{\epsilon_2} - C_{\epsilon_1})$ is well known. This a priori test is consistent with the fact that several corrections (e.g., Iacovides and Launder, 1995; Rodi and Mansour, 1993), introduced into the classical $\epsilon$-equation, or modifications of the model constants, did not show any significant improvement of the backflow intensity in our full SMC computations. Since $\epsilon$ is thought not to be responsible for the backflow and recovery discrepancy, we come back to other modeled terms; first to the transport model.

We tested this model by the new a priori technique. If just the $k$ equation is solved, with DNS data for $\epsilon$, then the only modeled term is the turbulent transport (see Eq. (1)). Solving just the $k$-equation gave results similar to those presented in Fig. 5(*b*). Surprisingly, the behavior of the transport model is excellent in this case (backstep at low Reynolds number). In fact, the only discrepancy that has been found concerns the secondary recirculation ($x/h = 0.1$ and 2) where a severe over-

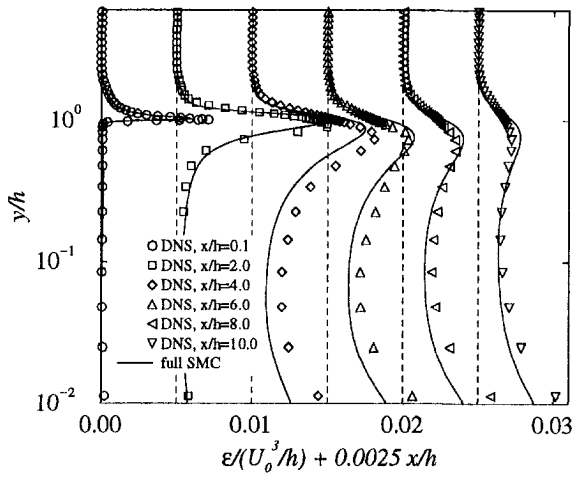


**Fig. 6(*a*) $\epsilon$ profiles, full computation**

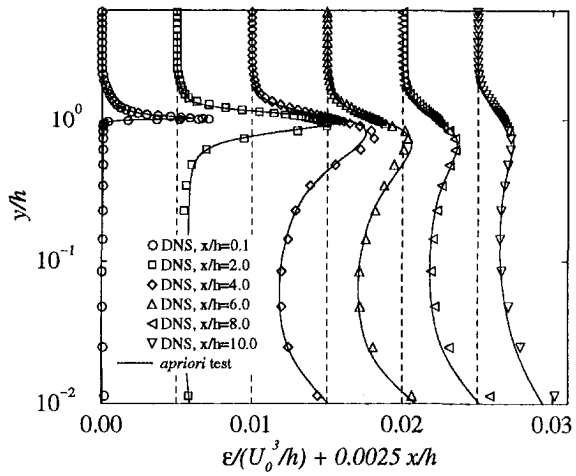


**Fig. 6(*b*) $\epsilon$ profiles, a priori test**

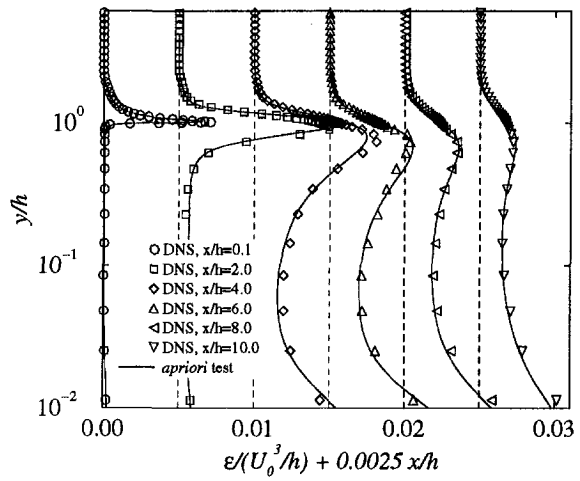


**Fig. 7(*a*)** $\epsilon$ **a priori profiles with** $U^{DNS}$, $k^{DNS}$, $\overline{u_i u_j}^{DNS}$ **and Eq. (3)**

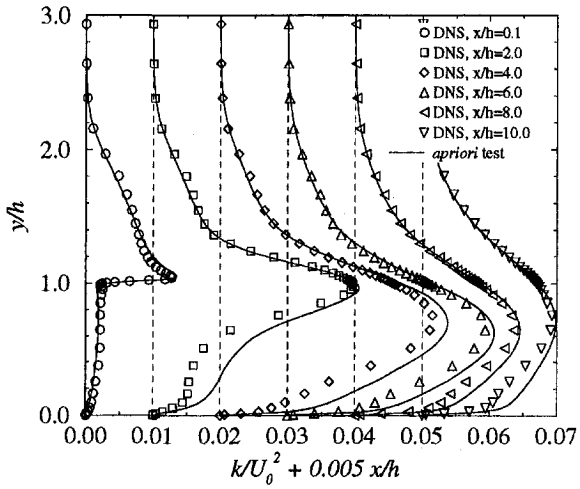


**Fig. 7(*b*)** *k* **a priori profiles without the extra-production term in Eq. (3)**

prediction has been obtained. The full computation presented in the previous section used $C_\mu = 0.22$; this behavior in the secondary recirculation is not improved by modifying $C_\mu$. Hence, the usual gradient transport formula performs very well in the shear layer but over-predicts the turbulence in the near-wall region, especially in the secondary recirculation region. We tried to improve the Daly-Harlow model by including a dependence on gradients of the mean flow, but even when more accurate *k*-profiles in the secondary bubble were obtained by the a priori test, the full computation did not show any improvement in the $C_f$ distribution.

In conclusion, these results lead us to believe that both the *k* and $\epsilon$ equations of the Second Moment Closure approach represent the physics of the flow quite well (at least in this case) and that the backflow and recovery problems come from other equations of the model, i.e., the Reynolds-stress transport equations.

The same kind of a priori test was repeated for each $\overline{u_i u_j}$-equation and its associated elliptic relaxation operator for the pressure-strain correlation. We have already explained the interest in doing such tests: the full RANS computation does not isolate faults in the modeling. Indeed, the $\overline{uv}$-profiles obtained through the full computation seem to be quite good whereas the a priori test (with $\overline{u^2}$, $\overline{v^2}$, $U$, $V$, $k$ and $\epsilon$ fixed to their DNS value) shows an over-prediction of the gradient—$\partial_y \overline{uv}$ near the wall (Fig. 8). This erroneous gradient has a crucial influence on mean flow prediction.

The corresponding results for $\overline{v^2}$ are portrayed in Fig. 9. The computation of $\overline{u^2}$ will not be shown, but the levels of agreement to data are similar to Fig. 9. In both cases the a priori solution is much better than was found for $\overline{uv}$. Also, Fig. 9 shows again the interest of this a priori testing technique. The full computation predicts a sever under-estimation of $\overline{v^2}$ in the whole domain, and especially in the recirculation. One might think that the $\overline{v^2}$-equation needs to be improved, whereas the a priori test shows that once all the other variables are well predicted, there is no need of modifications at all.

The mean momentum budgets show that the dominant turbulent forces are $-\partial_y \overline{uv}$ and $-\partial_y \overline{v^2}$. These terms, computed with the a priori tests, are shown in Figure 10. The normal stress gradient, $\partial_y \overline{v^2}$ (Fig. 10(*a*)), which appears in the *V*-equation, has a peculiar behavior at the corner of the step ($x = 0.1$, $y = 1$), but this deficiency seems to stay local and to have little influence on the rest of the domain; the kink that is observed here has not been transported downstream ($x/h \geq 2$). With the exception of this problem, $\overline{v^2}$ is accurately predicted. The only other discrepancy can be found near the wall before the reattachment point, at $x/h = 4$ and 6. This should not directly affect the mean flow because at this location the flow is nearly parallel to the wall, $V = 0$.

Figure 10(*b*) shows the a priori turbulent force acting in the *U*-momentum equation. At locations $x/h = 4$, 6 and 8 and $y < 0.15$, this force is over-predicted by almost a factor of 2. These locations are near the reattachement point. In the backflow re-

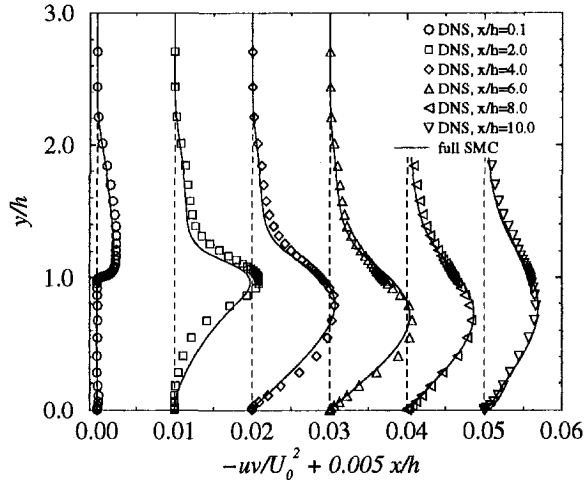


**Fig. 8(*a*)** $-\overline{uv}$ **profiles, full computation**

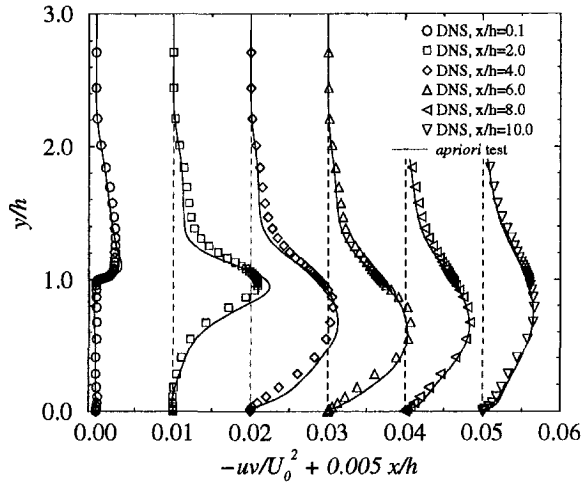


**Fig. 8(*b*)** $-\overline{uv}$ **profiles, a priori test**

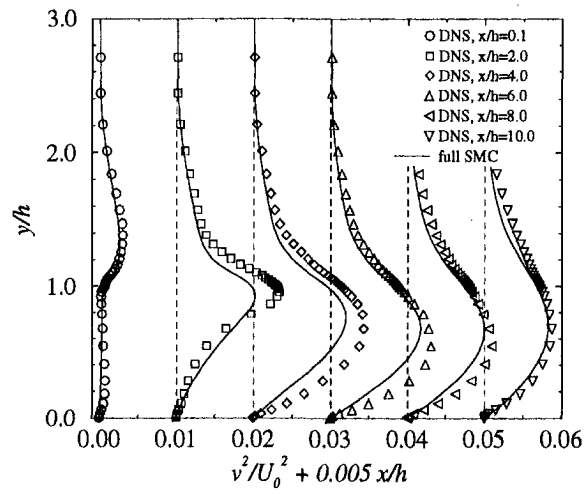


Fig. 9(*a*) $\overline{v^2}$ profiles, full computation

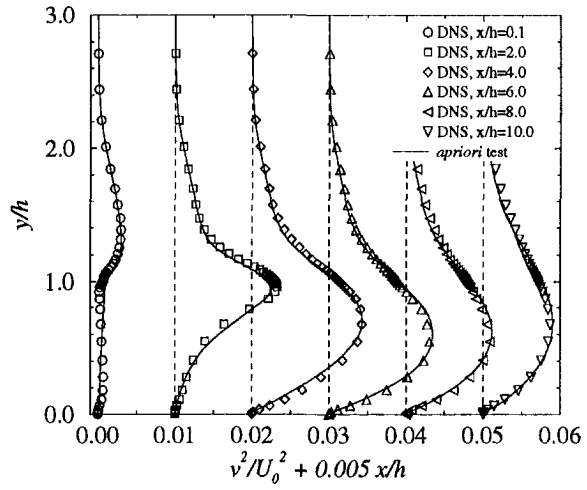


Fig. 9(*b*) $\overline{v^2}$ profiles, a priori test

gion $U$ is negative and the turbulent force, $-\partial_y\overline{uv}$, acts to slow down the flow. Thus the over-prediction by a factor of 2 could explain the severe under-prediction of backflow we obtained with the full SMC computation. We should remark that this a priori test was performed with $\epsilon_{12}^{\mathrm{DNS}}$; this shows that anisotropy of the dissipation tensor has little effect. It does not seem that a model of dissipation anisotropy is warranted (in fact, we performed computations with one such model, but the results were similar to those presented herein).

A parametric study on the constants of the SSG pressure-strain model was performed: whatever the modifications attempted, the a priori test on the $\overline{uv}$-equation still showed an over-prediction of $-\partial_y\overline{uv}$ in the backflow region. These various tests led to the sentiment that this time the transport model might be in fault.

Hanjalic and Launder (1972) arrived at their gradient transport expression by neglecting the convection, diffusion and production terms in the third moment transport equation. Daly and Harlow (1970) only retained terms involving $\partial_l\overline{u_iu_j}$ in the $\overline{u_iu_ju_l}$ equation, with other terms acommodated by modifying the constant $C_\mu$. The appendix uses the simpler, Daly-Harlow, form (computations were done also with the Hanjalic-Launder form, but we get similar results, i.e., the turbulent force stayed twice too high in the backflow region). We tried to modify this transport model by introducing a dependence on the gradient of mean flow:

$$T_{ij} = T_{ij}^{DH} - \frac{3}{4}\frac{\partial}{\partial x_k}\left\{(C_\mu T)^2 P_{il}\frac{\partial\overline{u_ju_k}}{\partial x_l} + (C_\mu T)^2 P_{jl}\frac{\partial\overline{u_iu_k}}{\partial x_l}\right\} \quad (4)$$

$P_{ij}$ is the production of $\overline{u_iu_j}$ and $T_{ij}^{DH}$ is the classical Daly-Harlow model (cf. Appendix).

Figure 10 includes the results obtained with this new model. An improvement in the prediction of both $-\partial_y\overline{uv}$ (decrease of the over-prediction of the turbulent force in the backflow) and $-\partial_y v^2$ in the near-wall backflow region can be seen, without significant modifications to the profiles in the rest of the domain. When this new model was implemented into the whole set of equations (keeping the Daly-Harlow model for $\epsilon$ since it has given excellent results), a significant improvement in the $C_f$ distribution was obtained (Fig. 2($a$)). This shows that the a priori tests and the subsequent analysis are consistent with the full SMC computation. The discrepancy of the minimum friction coefficient was reduced by 50 percent without any damage to the recirculation length prediction. Such an improvement was not obtained with other modifications including additive terms in the $\epsilon$-equation, changes of the pressure-strain model and parametric variations of the model constants. Even though the profiles of $\overline{uv}$ in the recovery were not affected by this new model during the a priori test, the improvement in the backflow region improved the friction coefficient and the $U$-profiles in the recovery as well (Fig. 2($b$)).

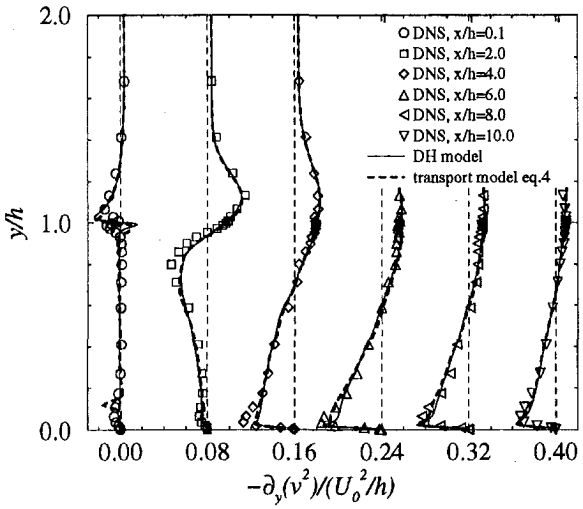


Fig. 10(*a*) A priori Reynolds force $-\partial_y\overline{v^2}$ profiles

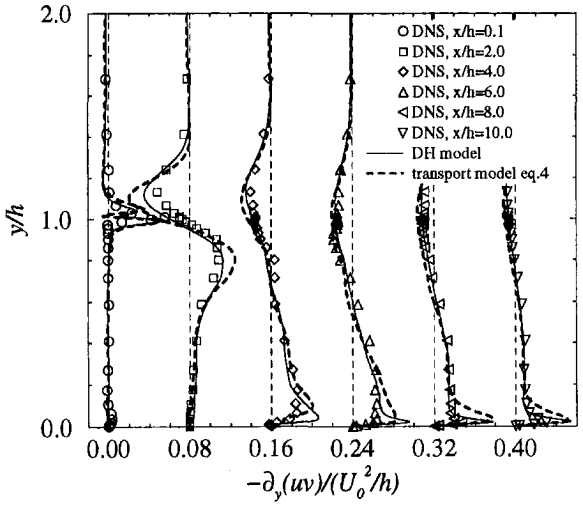


Fig. 10(*b*) A priori Reynolds force $-\partial_y\overline{uv}$ profiles

The maximum backflow is still under-predicted and needs some cure. In fact, this new model only affects the near-wall region of the flow, which becomes thinner at higher Reynolds number. We tried the new transport model in high-Re case, where the recovery discrepancy was more pronounced. Once again, the friction coefficient distribution, which shows a similar relative under-prediction by a factor of 2 of the minimum peak, was improved by 50 percent in the backflow, but this improvement could no longer be seen in the $U$-profiles and the solution still showed a too slow recovery.

Over all, the present results explain the interest in using this new a priori testing technique to study the solution properties of RANS models. The new transport model illustrated how shortcomings that are identified might generate ideas for improving turbulence models.

## 5 Conclusion

A full Second Moment Closure computation has been carried out for evaluating the turbulent flow over a backward-facing step at low Reynolds number (Re = 5,100). The model, including elliptic relaxation of pressure-strain for taking into account the non-local effects of pressure near to walls, has previously been calibrated solely with channel flow and zero pressure gradient turbulent boundary layer data at various Reynolds numbers; it has been directly applied to the backstep without any modification. The results show a very good prediction of the recirculation length, but an under-prediction of the backflow by a factor of 2. The recovery has been seen also to be too slow.

An analysis of the corresponding DNS database proved that the main bubble is definitely turbulent, even at this low Reynolds number. A new technique of a priori testing with DNS data has been developed; it consists, basically, in evaluating the accuracy of each equation of the model by solving one variable while fixing all the others to their DNS values. It came out that both Daly-Harlow transport model for $k$, and the $\epsilon$-equation do surprisingly well, to the contrary of what is generally thought in the literature.

In fact, the main problem comes from the $\overline{uv}$-equation, which gives an over-prediction of the turbulent force ($-\partial_y\overline{uv}$), which is acting as slowing down the backflow, by a factor of 2 in the middle of the recirculation. We attempted a modification of the transport Daly-Harlow model, by including terms involving the gradient of mean flow. Both a priori tests and full computation showed an improvement of the near-wall behavior of the model; 50 percent of the $C_{f_{min}}$ discrepancy in the backflow has been cured without deteriorating the excellent prediction of the recirculation length.

## Acknowledgments

S.P. thanks Electricité de France for their financial support; P.D. acknowledges support from the Office of Naval Research, Dr. L. P. Purtell, program manager.

## References

Daly, B., and Harlow, F., 1970, "Transport Equations in Turbulence," *Physics of Fluids,* Vol. 13, No. 11, pp. 2634–2649.

Durbin, P., 1993, "A Reynolds-Stress Model for Near-Wall Turbulence," *Journal of Fluid Mechanics,* Vol. 249, pp. 465–498.

Durbin, P. A., and Laurence, D., 1996, "Nonlocal Effects in Single Point Closure," Turbulence Research Associates-96 meeting, Seoul Korea.

Hanjalic, K., and Launder, B. E., 1972, "A Reynolds Stress Model of Turbulence and Its Application to Thin Shear Flows," *Journal of Fluid Mechanics,* Vol. 52, pp. 609–638.

Hanjalic, K., 1994, "Advanced Turbulence Closure Models: A View of Current Status and Future Prospects," *International Journal of Heat and Fluid Flow,* Vol. 15, No. 3, pp. 178–203.

Hanjalic, K., 1996, "Some Resolved and Unresolved Issues in Modeling Non Equilibrium and Unsteady Turbulent Flows," *Engineering Turbulence Modeling and Measurements,* W. Rodi and G. Bergeles, eds., Elsevier Publ, Vol. 3, pp. 3–18.

Iacovides, H., and Launder, B. E., 1995, "Computational Fluid Dynamics Applied to Internal Gas-Turbine Blade Cooling: A Review," *International Journal of Heat and Fluid Flow,* Vol. 16, pp. 454–470.

Jovic, S., and Driver, D., 1995, "Reynolds Number Effect on the Skin Friction in Separated Flows Behind a Backward-Facing Step," *Experiments in Fluids,* Vol. 18.

Le, H., Moin, P., and Kim, J., 1997, "Direct Numerical Simulation of Turbulent Flow Over a Backward-Facing Step," *Journal of Fluid Mechanics,* Vol. 330, pp. 349–374.

Parneix, S., Laurence, D., and Durbin, P., 1996, "Second moment closure analysis of the backstep flow database," *Proceedings of the CTR 1996 Summer Program,* Stanford University, Vol. 6, pp. 47–62.

Rodi, W., and Mansour, N. N., 1993, "Low Reynolds Number $k-\epsilon$ Modeling With the Aid of Direct Simulation Data," *Journal of Fluid Mechanics,* Vol. 250, pp. 509–529.

Rogers, S. E., and Kwak, D., 1990, "Upwind Differencing Scheme for the Time-Accurate Incompressible Navier-Stokes Equations," *AIAA Journal,* Vol. 28, pp. 253–262.

Speziale, C. G., Sarkar, S., and Gatski, T. B., 1991, "Modeling the Pressure-Strain Correlation of Turbulence: An Invariant Dynamical Systems Approach," *Journal of Fluid Mechanics,* Vol. 227, pp. 245–272.

Wizman, V., Laurence, D., Durbin, P. A., Demuren, A. O., and M. Kanniche, 1996, "Modeling Near Wall Effects in Second Moment Closures by Elliptic Relaxation," *International Journal of Heat and Fluid Flow,* 17, 255–266.

# APPENDIX

## Second Moment Closure With Elliptic Relaxation

The Reynolds stress transport equation is written as:

$$D_t\overline{u_iu_j} = P_{ij} + \wp_{ij} - \overline{u_iu_j}\frac{\epsilon}{k} + T_{ij} + \nu\nabla^2\overline{u_iu_j} \qquad (A.1)$$

with

$$P_{ij} = -\overline{u_iu_k}\partial_kU_j - \overline{u_ju_k}\partial_kU_i$$
$$\wp_{ij} = -\overline{u_i\partial_jp} - \overline{u_j\partial_ip} - \left(\epsilon_{ij} - \overline{u_iu_j}\frac{\epsilon}{k}\right) + \tfrac{2}{3}\overline{u_k\partial_kp}\,\delta_{ij}$$
$$T_{ij} = -\partial_k(\overline{u_ku_iu_j} + \tfrac{2}{3}\overline{u_kp}\,\delta_{ij}) \qquad (A.2)$$

The term $\wp_{ij}$ differs from the usual pressure-strain $\phi_{ij}$ since it includes a deviatoric dissipation tensor in the form

$$\wp_{ij} = \phi_{ij} - \left(\epsilon_{ij} - \overline{u_iu_j}\frac{\epsilon}{k}\right) \qquad (A.3)$$

The following neutral formulation for the elliptic relaxation is now invoked (Durbin and Laurence, 1996):

$$f_{ij} - L^2\nabla^2f_{ij} = \frac{L\wp^h_{ij}}{k} \qquad (A.4)$$

with $\wp_{ij} \equiv kf_{ij}/L$. For homogeneous turbulence $\wp_{ij}$ in Eq. (A.4) reduces to $\wp^h_{ij}$, for which any standard redistribution model $\phi^h_{ij}$ can be used. The SSG rapid model is

$$\wp^h_{ij_{rapid}} = -C_2dev(P_{ij}) - C_3dev(D_{ij}) - C_skS_{ij} \qquad (A.5)$$

where "$dev$" denotes the deviatoric operator: $dev(P_{ij}) = P_{ij} - \frac{1}{3}P_{kk}\delta_{ij}$ The coefficients are:

$$C_2 = 0.4125;\ C_3 = 0.2125;\ C_s = \tfrac{1}{30} + 0.65\sqrt{A_2} \qquad (A.6)$$

The slow term is of the form

$$\wp^h_{ij_{slow}} = -[C_1a_{ij} + C_1'dev(a_{ik}a_{kj})]\frac{k}{T} \qquad (A.7)$$

with

$$a_{ij} = dev(\overline{u_iu_j})/k \quad \text{and} \quad A_2 = a_{ij}a_{ij}. \qquad (A.8)$$

The model coefficients are

$$C_1 + 1 = \left[ 1.7 + 0.9 \frac{\mathcal{P}}{\epsilon} \right], \; C_1' = -1.05. \qquad \text{(A.9)}$$

The time scale, $T$, is defined as:

$$T = \sqrt{\frac{k^2}{\epsilon^2} + 36 \frac{\nu}{\epsilon}} \qquad \text{(A.10)}$$

The length scale $L$ also is prevented from going to zero at the wall by using the Kolmogorov scale as a lower bound:

$$L = C_L \sqrt{\frac{k^3}{\epsilon^2} + C_\eta^2 \frac{\nu^{3/2}}{\epsilon^{1/2}}} \qquad \text{(A.11)}$$

Lastly, the Daly-Harlow expression for the turbulent diffusion is used:

$$T_{ij} = \partial_l (C_\mu \overline{u_l u_m} T \partial_m \overline{u_i u_j}) \qquad \text{(A.12)}$$

The remaining constants used in our computations are:

$$C_\mu = 0.22, \; \sigma_\epsilon = 1.5, \; C_L = 0.1, \; C_\eta = 230,$$

$$C_{\epsilon_1} = 1.44, \; C_{\epsilon_2} = 1.83 \qquad \text{(A.13)}$$